(4)

David Taylor Research Center

Bethesda, MD 20084-5000

DTRC/SHD-1298-02 December 1989

Ship Hydromechanics Department

Departmental Report

EXPERIMENTS OF THE DARPA SUBOFF PROGRAM

by

Thomas T. Huang

Han-Lieh Liu

Nancy C. Groves

Approved for public release;
Distribution is unlimited.

DTRC/SHD-1298-02 EXPERIMENTS OF THE DARPA SUBOFF PROGRAM

MAJOR DTRC TECHNICAL COMPONENTS

CODE 011 DIRECTOR OF TECHNOLOGY, PLANS AND ASSESSMENT

12 SHIP SYSTEMS INTEGRATION DEPARTMENT

14 SHIP ELECTROMAGNETIC SIGNATURES DEPARTMENT

15 SHIP HYDROMECHANICS DEPARTMENT

16 AVIATION DEPARTMENT

17 SHIP STRUCTURES AND PROTECTION DEPARTMENT

18 COMPUTATION, MATHEMATICS & LOGISTICS DEPARTMENT

19 SHIP ACOUSTICS DEPARTMENT

27 PROPULSION AND AUXILIARY SYSTEMS DEPARTMENT

28 SHIP MATERIALS ENGINEERING DEPARTMENT

DTRC ISSUES THREE TYPES OF REPORTS:

1. **DTRC reports, a formal series,** contain information of permanent technical value. They carry a consecutive numerical identification regardless of their classification or the originating department.

2. **Departmental reports, a semiformal series,** contain information of a preliminary, temporary, or proprietary nature or of limited interest or significance. They carry a departmental alphanumerical identification.

3. **Technical memoranda, an informal series,** contain technical documentation of limited use and interest. They are primarily working papers intended for internal use. They carry an identifying number which indicates their type and the numerical code of the originating department. Any distribution outside DTRC must be approved by the head of the originating department on a case-by-case basis.

NDW-DTNSRDC 5602/51 (Rev 2-88)

UNCLASSIFIED
SECURITY CLASSIFICATION OF THIS PAGE

REPORT DOCUMENTATION PAGE

1a. REPORT SECURITY CLASSIFICATION: Unclassified	1b. RESTRICTIVE MARKINGS
2a. SECURITY CLASSIFICATION AUTHORITY	3. DISTRIBUTION / AVAILABILITY OF REPORT: Approved for public release; distribution is unlimited.
2b. DECLASSIFICATION / DOWNGRADING SCHEDULE	
4. PERFORMING ORGANIZATION REPORT NUMBER(S): DTRC/SHD-1298-02	5. MONITORING ORGANIZATION REPORT NUMBER(S)
6a. NAME OF PERFORMING ORGANIZATION: David Taylor Research Center; 6b. OFFICE SYMBOL (If applicable): Code 1542	7a. NAME OF MONITORING ORGANIZATION
6c. ADDRESS (City, State, and Zip Code): Bethesda, MD 20084-5000	7b. ADDRESS (City, State, and Zip Code)
8a. NAME OF FUNDING / SPONSORING ORGANIZATION: DARPA; 8b. OFFICE SYMBOL (If applicable)	9. PROCUREMENT INSTRUMENT IDENTIFICATION NUMBER
8c. ADDRESS (City, State, and Zip Code): STP Support Office, 1515 Wilson Blvd., Suite 705, Arlington, VA 22209	10. SOURCE OF FUNDING: PROGRAM ELEMENT NO. 63569N; PROJECT NO.; TASK NO. S1974030; WORK UNIT ACCESSION NO. DN509067

11. TITLE (Include Security Classification)

EXPERIMENTS OF THE DARPA SUBOFF PROGRAM

12. PERSONAL AUTHOR(S): Thomas T. Huang, Han-Lieh Liu, Nancy C. Groves

13a. TYPE OF REPORT	13b. TIME COVERED	14. DATE OF REPORT (Year, Month, Day)	15. PAGE COUNT
Departmental	FROM_____ TO_____	1989, December	

16. SUPPLEMENTARY NOTATION

17. COSATI CODES			18. SUBJECT TERMS (Continue on reverse if necessary and identify by block number)
FIELD	GROUP	SUB-GROUP	DARPA SUBOFF, pressure coefficient, mean velocity, flow measurements, shear stress, wake profile, Reynolds stress,

19. ABSTRACT (Continue on reverse if necessary and identify by block number)

Experimental measurements of the flow field of an axisymmetric body, bridge fairwater, four identical symmetric stern appendages, and two ring wings with ring wing support struts will be made in the David Taylor Research Center (DTRC) Anechoic Flow Facility (AFF) and deep-water towing basins (TMB) and Tracor Hydronautics Ship Model Basin (HSMB). The experimental data will be used to assess the current Computational Fluid Dynamics capability for the Defense Advanced Research Projects Agency (DARPA) SUBOFF Project. Experimental facilities and techniques are presented, and the contents of the experiments are outlined. This information together with the geometric characteristics of DARPA SUBOFF models is intended for use by both the model test engineers and the CFD engineers.

20. DISTRIBUTION / AVAILABILITY OF ABSTRACT: ☒ UNCLASSIFIED/UNLIMITED ☐ SAME AS RPT ☐ DTIC USERS	21. ABSTRACT SECURITY CLASSIFICATION: Unclassified
22a. NAME OF RESPONSIBLE INDIVIDUAL: Thomas T. Huang	22b. TELEPHONE (Include Area Code): 301-227-1325; 22c. OFFICE SYMBOL: Code 1542

DD FORM 1473, 84 MAR — 83 APR edition may be used until exhausted. All other editions are obsolete.

SECURITY CLASSIFICATION OF THIS PAGE
UNCLASSIFIED

CONTENTS

FIGURES

TABLES

NOMENCLATURE

A_{un}	cosine coefficient for axial velocity component
A_{vn}	cosine coefficient for radial velocity component
A_{wn}	cosine coefficient for tangential velocity component
B_{un}	sine coefficient for axial velocity component
B_{vn}	sine coefficient for radial velocity component
B_{wn}	sine coefficient for tangential velocity component
C_p	pressure coefficient $= \frac{P-P_{ref}}{1/2\ \rho\ U^2_{ref}}$
C_τ	wall shear stress coefficient $= \frac{\tau_w}{1/2\ \rho\ U^2_{ref}}$
h	non-uniform grid spacing
J	probe number used in the time-varying harmonic study
K	integer
L	model length, turbulence length scale
N	harmonics number
P_{ref}	pressure at x/L = 0.85 and $r/R_{max} = 2.7$, $\theta = 0$ degrees
r	ratio of lengths of any two radial distances in defining the boundary layer thickness
R_{max}	maximum body radius
R_λ	turbulence Reynolds number
S	the power spectral density amplitude
t	time
T	period in time-varying harmonics
U_o	free stream velocity
U_{ref}	reference velocity at x/L = 0.875 and $r/R_{max} = 2.7$, $\theta = 0$ degrees
u_x	mean axial velocity component, positive downstream
u'_x	turbulence velocity in the axial direction
v_r	mean radial velocity component, positive outward from center
v'_r	turbulence velocity in the radial direction
w_θ	mean tangential velocity component, positive counter-clockwise when viewing the model from stern to bow
w'_θ	turbulence velocity in the θ direction
x	axial coordinates, positive downstream

NOMENCLATURE (continued)

α	angle of attack for the model, pitch
β	angle of attack for the model, drift
γ	angle of attack for the model sternplane
δ_r	local boundary layer thickness
ε	turbulence energy dissipation
η	Kolmogorov length scale
θ	angle defined in the polar coordinates
λ	microscale turbulence
ν	eddy viscosity
ρ	density
τ	turbulence time scale
τ_w	wall shear stress
Ω	the power spectral density phase angle

ABSTRACT

Experimental measurements of the flow field of an axisymmetric body, bridge fairwater, four identical symmetric stern appendages, and two ring wings with ring wing support struts will be made in the David Taylor Research Center (DTRC) Anechoic Flow Facility (AFF) and deep-water towing basins (TMB) and Tracor Hydronautics Ship Model Basin (HSMB). The experimental data will be used to assess the current Computational Fluid Dynamics capability for the Defense Advanced Research Projects Agency (DARPA) SUBOFF Project. Experimental facilities and techniques are presented, and the contents of the experiments are outlined. This information together with the geometric characteristics of DARPA SUBOFF models is intended for use by both the model test engineers and the CFD engineers.

ADMINISTRATIVE INFORMATION

This work was funded under DARPA, Task Area S1974-030, Program Element 63569N, with internal DTRC Work Unit Numbers 1-1542-123, 1-1542-126 and 1-1542-127.

INTRODUCTION

The Submarine Technology Program (STP) Office of the Defense Advanced Research Project Agency (DARPA) has funded a concerted and coordinated Computational Fluid Dynamics (CFD) Program to assist in the development of advanced underwater bodies. The flow over an entire appended body during level flight is characterized by thick boundary layers, vortical flow structures generated by hull/appendage junctures, and turbulent wakes. The spatial and time-varying harmonics of the flow into the propulsor significantly affect propulsor noise. Flow separation will occur during various maneuvers, especially during severe maneuvers when the vortices shed from the fairwater and hull (cross-flow open separation) will interact with the stern, stern appendages, and propulsor to generate out-of-plane forces and moments.

Limited experimental data for CFD validation purposes have been obtained during the past 15 years. They are (1) thick stern boundary layer data for various axisymmetric configurations [1-6], (2) appendage/flat-plate juncture flow data [7,8], and (3) flow data for a curved body, which simulates qualitatively the flow features of a turning body [9]. Experimental data for the flow field over an entire appended body are seriously lacking and the validation of CFD numerical methods for submarine design

applications cannot be adequately accomplished. The DARPA SUBOFF project will provide a forum for the CFD community to compare the numerical predictions of the flow field over an axisymmetric hull model with and without various typical appendage components with experimental data. The CFD predictions of flow fields of typical configurations will be made without the prior knowledge of the actual experimental data. Experimental and computational comparisons can then be made to demonstrate the current CFD capability on design problems relevant to STP problem areas. The ultimate goal of the SUBOFF project is to acquire a fully-matured CFD capability that is user-friendly, cost effective and fully verified by comparison with detailed experimental data.

The role of CFD in conventional ship design and model evaluation has been summarized by Morgan and Lin [10]. The current capabilities and future directions in CFD as applied to aerospace engineering [11] have been assessed periodically by a committee under the auspices of the National Research Council of the United States. The state-of-the-art of both the experimental and CFD techniques as related to ship hull and propulsor design and performance prediction has been addressed by Morgan and Lin [12]. The influence of CFD on aerospace experimental facilities [13] has been reported by a committee of the National Research Council. Various CFD techniques have been developed and applied to solve certain aspects of submarine hydrodynamic problems in the past. A partial list of the relatively mature current CFD techniques, which are cost-effective and reliable follows:

(1) Software for the design of conventional propulsors by lifting line theory and lifting surface theory.

(2) Software for the prediction of propulsor performance (mean thrust, torque and efficiency) by inverse lifting surface theory and a surface panel method with viscous correction.

(3) Software for the prediction of the difference of radial distribution of circumferentially-averaged inflow into the propulsor between the model and full scale using a viscous-inviscid interactive boundary-layer theory.

(4) Software for the prediction of the propeller/hull interaction (thrust deduction) by a surface panel method.

(5) Software for the prediction of the laminar boundary-layer over the bow using laminar boundary-layer theory and prediciton of transition from laminar to turbulent flow on the forebody using an empirical spatial amplication factor in conjunction with linear boundary-layer instability theory.

(6) Software for the prediction of turbulent boundary layers over the forebody and most of the parallel middle body using turbulent boundary-layer computational techniques.

As the flow approaches the stern, the boundary layer thickness quickly increases, viscous-inviscid flow interaction becomes pronounced, turbulence reacts to the change in mean flow, and conventional thin boundary-layer turbulence modeling is no longer directly applicable. Since the stern control surfaces are

generally immersed in this thick boundary layer, the numerical capability to predict the control effectiveness of the stern control surfaces and their adverse effect on the flow into the propulsor is rather limited. In addition, a large fairwater can generate a turbulent junction vortex around the nose of the fairwater/hull intersection and a pair of vortices which trail downstream into the propulsor. The low frequency unsteadiness around the fairwater and the vortex-induced spatial nonuniformity of the flow into the propulsor are of major concern. The CFD capability to predict the flow nonuniformity at the propulsor location, due to the fairwater and stern control surfaces, is seriously lacking. This nonuniformity is the major source of propulsor noise. The CFD capability to predict the propulsor noise arising from the small spatial variation and low-frequency unsteadiness of the propulsor inflow is also not well developed. Furthermore, in order to develop a highly maneuverable submarine, a time-dependent CFD capability to predict the out-of-plane forces and moments due to the interaction of vortices shed from the fairwater, hull, stern appendages and propulsor during various maneuvers must also be developed.

Eight simple representative configurations were selected for the experimental SUBOFF program. They include:

(1) a bare axisymmetric body,

(2) an axisymmetric body with fairwater,

(3) an axisymmetric body with four identical stern appendages,

(4) an axisymmetric body with fairwater at zero drift and varying angle of attack,

(5) an axisymmetric body with fairwater at zero angle of attack and varying drift,

(6)-(7) an axisymmetric body with two different stern ring wings, and

(8) an axisymmetric body with both fairwater and four stern appendages.

The flow velocities, forces, moments and pressure distributions on the axisymmetric body and forces, moments and pressure distributions on one of the stern appendages at steady body angles of attack and drift will provide the validation of current CFD capability for STP. The proposed first phase of SUBOFF is designed to accelerate the maturity of current CFD capability for submarine applications. The geometric characteristics of the eight SUBOFF configurations are detailed in Reference 14.

The following sections present the experimental facilities and techniques to be used and the content of the experiments to be performed.

EXPERIMENTAL FACILITIES AND TECHNIQUES

A portion of the experimental investigation of the eight DARPA SUBOFF model configurations will be conducted in the DTRC AFF with Model No. 5471. As shown in Fig. 1, the wind tunnel has a closed jet test section that is 8 ft (2.4 m) square and 13.75 ft (4.19 m) long. The corners have 1'-9" x 1'-9" (0.534 x 0.534 m) fillets which are carried through the contraction. Allowance for boundary layer growth along the tunnel is made by tapering the corner fillets, starting from 1'-9" x 1'-9" (0.534 x 0.534 m) at the test section entrance to 1'-8" x 1'-8" (0.509 x 0.509 m) at the test section exit. The test section is followed by a large acoustically-lined chamber 23.5 ft (7.16 m) square, normal to the flow, and 21 ft (6.40 m) long. The forebody and most of the parallel middle body will be located in the closed-jet test section, and the afterbody will be protruding into the open-jet anechoic chamber shown in Fig. 2a. The model arrangement, shown in Fig. 2b, will reduce the tunnel blockage effect on the stern flow to a minimum. The major purpose of the SUBOFF experiments is to obtain high-quality data on the axisymmetric and three-dimensional stern flows of the eight model configurations.

Two NACA-0015 struts are required to support the model. The two supporting struts have a 6" (15 cm) chord. Most of the experimental data will be for flow on the upper surface of the model where strut effects should be minimal. The location of the two struts is shown in Fig. 2b. All the experiments will be conducted at a Reynolds number, based on model length, of 1.2×10^7. It should be noted that the full-scale Reynolds number of interest is 10^8 to 10^9. The CFD capability verified at a Reynolds number of 1.2×10^7 must readily be extended to Reynolds numbers of 10^8 to 10^9 in order to meet the DARPA STP objectives. The installation and pretest analyses of the blockage of the model in the wind tunnel will be presented in a separate report.

The DTRC AFF will be used to obtain stern flows of:

(1) the bare axisymmetric body at zero angle of attack and drift,
(2) the axisymmetric body with a conventional fairwater at zero body angle of attack and drift,
(3) the axisymmetric body with four identical stern appendages at zero body angle of attack and drift,
(4) the axisymmetric body with a fairwater at a body angle of attack (2° bow up) and zero angle of drift,
(5) the axisymmetric body with a fairwater at a body angle of drift (2° to starboard) and zero angle of attack,
(6) the axisymmetric body at zero body angle of attack and drift with ring wing 1,
(7) the axisymmetric body at zero body angle of attack and drift with ring wing 2, and
(8) the axisymmetric body with a fairwater and four identical stern appendages at zero body angle of attack and drift.

The maximum body angle of attack or drift in the DTRC AFF will be limited to two degrees. In order to measure the flows at larger angles of attack and drift (up to 18 degrees), as might be expected during severe maneuvers, larger wind tunnels and towing tanks must be used to avoid the adverse blockage effect. The DTRC deep water model basin (TMB) and Tracor Hydronautics Ship Model Basin (HSMB) were selected to obtain the force/moment and pressure distributions on the axisymmetric body Model No. 5470 and the force/moment and pressure distributions on one of the appendages at various angles of attack and drift.

The TMB will be used to measure the forces and moments of the axisymmetric body, with and without the bridge fairwater and stern appendages, the stern appendages alone, and the two ring wings. This model basin is 51 ft (15.54 m) wide and 22 ft (6.70 m) deep. The depth of submergence of the model is 9 ft (2.74 m). Experiments will be performed for a range of body angles of attack (-8 to +18°) and body angles of drift (-4 to +18°). Two vertical struts, as shown in Figs. 3a and 3b, will be used to tow the model. The longitudinal spacing between the centerlines of the struts is 6 ft (1.83 m). Each strut will be attached to the model through a set of three 4-inch block gages which measure the longitudinal, transverse and normal forces on the model. A gimbal between the three gages and the towing strut make it possible to determine the yawing and pitching moments. A five strain gage instrumented stock attached to one of the stern appendages will be used to measure the normal force, longitudinal force coefficients, spanwise center of pressure, and stock torque developed by the control surface.

Incremental resistance due to the appendages must be determined by an "appendage stripping" test in the TMB. The techniques to measure the pressure, wall shear stress and velocity measuring systems are briefly described below. The total resistance will be measured by a standard block gage for

(i) the axisymmetric body
(ii) the axisymmetric body with bridge fairwater
(iii) the axisymmetric body with four identical stern appendages,
(iv) the axisymmetric body with the two ring wings, and
(v) the axisymmetric body with the bridge fairwater and the four identical stern appendages.

A single strut, as shown in Fig. 4, will be used to tow the model. The bridge fairwater will be mounted upside down to avoid the interference effect of the towing strut on the drag. The depth of submergence of the model centerline is 11 ft (3.35 m) for the resistance measurements. The effect of turbulence stimulators on the appendages will also be measured.

The HSMB is 24 ft (7.32 m) wide, 12.76 ft (3.89 m) deep and 420 ft (128 m) long. The depth of submergence of the model is 6 ft (1.83 m). Two ogive struts (3-inch (0.82 m) chord and 1/8 inch (3.4 cm) thickness) will be used to support the model. The longitudinal spacing between the centerlines of the struts is 6 ft (1.83 m). A few additional force/moment measurements and appendage stripping tests will also be made for speeds up to 10 ft/s (3.05 m/s).

WIND TUNNEL PRESSURE MEASURING SYSTEM

The DARPA AFF Model No. 5471 will be used to provide surface pressure distributions at the junctures of the fairwater/hull and the appendage/hull. The pressure measuring system for the DARPA SUBOFF model is a mechanical pressure scanning system that connects all the model surface pressure taps, pitot-static tube taps, calibration pressure taps and free-stream static taps to silicone diaphragm differential pressure transducers. The five transducers are connected to signal conditioners and amplifiers inside the model, and the resulting signals connect to computer A/D converters. Pressure taps can be scanned at rates up to 10 per second. Connected to taps on the measurement side of each transducer are the reference pressure, calibration pressure and pitot tube static and total pressures. A high accuracy, temperature controlled pressure transducer located in the model is used as a standard and is connected to the five scanning pressure transducers for in situ calibration. Calibration pressure is externally controlled by a variable volume chamber in the control room. The system is designed to accurately measure pressure coefficients by comparing the differential pressure of each pressure tap on a transducer to the pitot tube dynamic pressure measured by the same transducer. This reduces bias type errors. Temperature drift errors are reduced by calibrating the transducers immediately before each run using the temperature controlled standard. The Model No. 5471 reference pressure will be the static pressure measured by the pitot probes in the anechoic test section chamber of the AFF.

WIND TUNNEL WALL SHEAR STRESS MEASURING SYSTEM

For measuring surface shear stress on the model, differential pressures will be measured with the pressure measuring system using obstacle blocks located on the downstream side of the pressure taps. The surface pressures will be measured with and without the obstacle blocks and the resulting pressure differences will be correlated to previous calibrations of the blocks using Preston tubes as a standard for shear stress measurement. The particular block shape that has been chosen is easy to apply adjacent to the pressure tap holes and produces a pressure rise that is comparable to the pressure rise produced by Preston tubes. The pressure rise in the range of 30-40% of the dynamic pressure will be easy to measure with the given pressure measuring system. The calibration procedures and uncertainty analyses of the pressure and wall shear stress measuring systems will be presented in a separate report.

WIND TUNNEL VELOCITY MEASURING SYSTEM

Velocity measurements in the boundary layer and wake will be made by using standard hot-film techniques. Single element, x-film and three-element probes will be used. The single-element probe will be used for thin boundary layers, the x-film probes for Reynolds stress in confined locations or when the flow is two-dimensional, and the three-element probes for the wake and thick stern boundary layer. For accurate and efficient measurement of the flow field of the DARPA submarine model configurations, a special hot-film velocity measuring system is being developed.

The measurement system will consist of three major subsystems: The hot-film probes and anemometers, the traverser, and the data acquisition system. The three subsystems will interact to provide accurate, efficient and easily documented data on the character of the flow. The shear number of measurements required for this experiment dictated a computer-controlled approach for acquiring, reducing and archiving the data.

The hot-film probes and anemometers have been carefully selected to match the particular types of measurements required for this experiment. Measurement in the thin boundary layers will require the use of single element probes aligned with the mean flow. Frequency response and voltage range will be optimized for the velocity range so that turbulence quantities can be measured accurately. For Reynolds stress measurements in regions where the flow is two-dimensional or in confined regions where the mean flow direction is known, x-film probes can be employed. For regions which are fully three-dimensional and do not have steep spatial velocity gradients, three-element probes of a new design having smaller measurement volume can be used. These will provide all three components of velocity and two components of Reynolds stress. At some locations, x-film and three-element probes will both be used to help determine uncertainty levels. Calibration of the various types of probes will be performed with the utmost care. All measurements will be compensated for temperature variations via a separate thermister thermometer. The calibration procedures, data reduction techniques and uncertainty analysis will be described in detail in a separate report.

The traverser system has been designed specifically for the particular measurements needed for this experiment. The axisymmetry of the model dictated a rotating movement for measurements at constant radius in the wake and stern boundary layers. Measurements of the thin boundary layer require a probe mount, which is supported locally and can move along a radial line. All such traversing will be computer controlled for efficiency in operations and in data recording. The circumferential distributions of axial, radial and tangential mean velocities at several radial locations at the propulsor plane are referred to by

naval architects as the wake survey. The angular position in this report is defined positive clockwise with respect to the upright (12 o'clock) position, viewing from the bow to the stern.

Data acquisition and reduction for hot-film measurements are computationally intensive and require an appropriately powerful computer for efficient and accurate operations. This is especially true for measurements using multiple three-element probes. Three-element probes require solution of three simultaneous calibration equations for each velocity realization, and multiple probes necessitate handling calibration equations and parameters for each probe separately. In addition, high speed data acquisition is required in order to obtain adequate frequency response, especially for multiple probes. The MASSCOMP MC5450 Scientific Laboratory System computer selected for this experiment meets all of these requirements and in addition runs the Unix operating system which allows access to numerous software utilities for efficient handling of the volumes of data to be acquired.

CONTENTS OF EXPERIMENTS

Experiments will be conducted mainly in the DTRC AFF and TMB. Additional experiments will be performed in the HSMB. The Reynolds number of 1.2×10^7, based on body length, will be kept for all the experiments. The experimental scope of the SUBOFF project is extremely large. Therefore, a cryptic notation has been adopted to identify the various tests. This brief notation identifies the test facility, the model configuration and the type and location of the data collected. The cryptic notation code is

A - B - C - D - E - F

A detailed explanation of the code is given in Table 1. As an example, the notation

$$\text{AFF-3-VP-0.978-r/R}_{max} = 0.60 \text{ - } -180^\circ < \theta < +180^\circ$$

would designate a test in the DTRC AFF (**A** = AFF); a model configuration of the axisymmetric body with four identical stern appendages at zero angle of attack and zero drift (**B** = 3); velocity profile data (**C** = VP); a normalized axial position x/L = 0.978 (**D** = 0.978); a normalized radial position $r/R_{max} = 0.60$ (**E** = $r/R_{max} = 0.60$); and a 360° measurement (**F** = $-180^\circ < \theta < +180^\circ$).

A brief outline of the tests involved will be described first. A detailed test plan will follow next.

DTRC AFF EXPERIMENT OUTLINE

The AFF experimental program involves the measurement of the flow quantities along the body (DTRC Model No. 5471). They are the three components of mean velocities and their turbulence intensities; two Reynolds stresses; boundary layer surveys along the upper meridian at five locations; static wall pressures along four meridians of the body; shear stresses at selected meridians/locations; and static pressure distributions in the near wake. In the wake survey experiments, both spatial and time varying harmonics will be studied.

Eight model configurations are tested. They are:

1. axisymmetric body at zero angle of attack and zero drift (designated as AFF-1-),
2. axisymmetric body with fairwater (designated as AFF-2-),
3. axisymmetric body with four identical stern appendages (designated as AFF-3-),
4. axisymmetric body with fairwater at angle of attack and zero drift (designated as AFF-4-),
5. axisymmetric body with fairwater at drift and zero angle of attack (designated as AFF-5-),
6. axisymmetric body with ring wing 1 (designated as AFF-6-),
7. axisymmetric body with ring wing 2 (designated as AFF-7-), and
8. axisymmetric body with fairwater and four identical stern appendages at zero angle of attack and zero drift (designated as AFF-8-).

DTRC AFF EXPERIMENT DETAILS

Detailed locations of the velocity and flow-field measurements are given below for each test condition. The circumferential angle, θ, is measured from the plane of the fairwater centerline, positive to port, zero at the fairwater and centered about the model longitudinal axis. A total number of about 15-20 measurement points across the stern boundary layer are required to define a velocity profile. Because the velocity profiles of turbulent flow close to the hull change rapidly, it is necessary to use a nonuniform measurement grid. One nonuniform grid is chosen in which the ratio of lengths of any two adjacent measurement intervals is constant; that is $r_i = r_{i-1} + h_i$ where $h_i = Kh_{i-1}$. The radial distance to the i^{th} measurement point is given by

$$r_i = r_0 + h_i \quad (K^i-1)/(K-1) \quad i = 1, 2, 3... J$$

where r_0 is the local hull radius. In all the boundary layer measurements, the first grid point from the hull is 0.01 δ_r and K = 1.2, where δ_r is the local boundary layer thickness. The radial locations of the axisymmetric boundary-layer measurement points are listed in Table 2.

The radial locations of the 3-D boundary-layer measurements of flows with various appendage components are selected in a similar manner, but with coarser grids.

1. Axisymmetric body (AFF-1-)

(a) In this configuration, only boundary layer and wake profiles need to be measured. Boundary layer measurements will be made at $\theta = 0°, \pm 45°$ and $\pm 90°$ at the following axial locations

(AFF-1-V-0.741)	
(AFF-1-V-0.781)	
(AFF-1-V-0.805)	$\theta = 0°, \pm 45°$
(AFF-1-V-0.840)	
(AFF-1-V-0.857)	
(AFF-1-V-0.904)	
(AFF-1-V-0.927)	$\theta = 0°, \pm 45°, \pm 90°$
(AFF-1-V-0.956)	
(AFF-1-V-0.978)	

Standard wake survey measurements will be made at the following axial locations:

(AFF-1-V-0.904)	$r/R_{max} = 0.45,\ 0.50,\ 0.60,\ 0.72,\ 0.92,\ 1.20$
(AFF-1-V-0.978)	
(AFF-1-V-1.040)	$r/R_{max} = 0.25,\ 0.30,\ 0.35,\ 0.40,\ 0.50,$
(AFF-1-V-1.096)	$0.60,\ 0.72,\ 0.92,\ 1.20,\ 2.00$
(AFF-1-V-1.200)	

Measurements include axial, radial and tangential mean (u_x/U_{ref}, v_r/U_{ref} and w_θ/U_{ref}) and turbulence ($\sqrt{u'^2_x}/U_{ref}$, $\sqrt{v'^2_r}/U_{ref}$ and $\sqrt{w'^2_\theta}/U_{ref}^2$) velocities, and axial-radial and axial-tangential Reynolds stresses ($\overline{-u'_x v'_r}/U_{ref}^2$ and $\overline{-u'_x w'_\theta}/U_{ref}^2$) across the planes designated.

(b) static wall pressure and shear stresses

(i) the pressure at the locations of the pressure taps given in Reference 14, designated by HU1 to HU21 for the upper meridian. Three additional pressure taps at lower, port and starboard meridians located at hull pressure tap stations 2, 5, 8, 11, 14 and 17 (AFF-1-P-).

(ii) the pressure on the hull around the fairwater/hull intersection region, designated in Reference 14 by FH1 to FH76 (AFF-1-P:FH)

(iii) the pressure on the hull around the stern appendage/hull intersection region, designated in Reference 14 by AH1 to AH41 (AFF-1-P:AH)

(iv) the wall shear stresses at the pressure tap locations given in Reference 14, designated by HU8 to HU21 for upper meridian and three other meridians at stations 8, 11, 14 and 17 (AFF-1-S-).

(c) static pressures in the upper meridian at the five velocity measurement planes (grid spacing same as 1a) designated as

(i) AFF-1-PP-0.840

(ii) AFF-1-PP-0.904

(iii) AFF-1-PP-0.978

(iv) AFF-1-PP-1.040

(v) AFF-1-PP-1.096

2. Body with fairwater (AFF-2-)

(a) The asymmetry in the flow due to the fairwater requires an additional radial measurement in the wake of the fairwater at $r/R_{max} = 1.6$. The standard wake survey at constant radius, $\theta \varepsilon (0, 360)$ degree will be made at the following axial locations and r/R_{max} values. Mean flow and turbulence velocities will be measured.

AFF-2-V-0.904 $r/R_{max} = 0.45,\ 0.50,\ 0.60,\ 0.72,\ 0.92,\ 1.2,\ 1.6,\ 2.0$

AFF-2-V-0.978

AFF-2-V-1.040 $r/R_{max} = 0.25,\ 0.30,\ 0.35,\ 0.40,\ 0.50,$

AFF-2-V-1.096 $0.60,\ 0.72,\ 0.92,\ 1.2,\ 1.6,\ 2.0$

AFF-2-V-1.200

For all of the above, $\Delta\theta$ will be 2.0 degrees except within $|\theta| < 20$ degrees when $\Delta\theta$ will be 1.0 degree. Measurements of the fairwater wake and the hull boundary layer interaction will be made at (AFF-2-V-0.840) $-45° \leq \theta \leq +45°$ with standard nonuniform grids of r/R_{max}.

(b) static pressure around the fairwater/hull intersection region with the bridge fairwater at an upright position (pressure tap locations FH1 to FH76 of Reference 14) designated as (AFF-2-P:FH-)

(c) static pressure at the pressure tap locations of FW1 to FW30 of the bridge fairwater as specified in Reference 14, designated as AFF-2-P:FW

(d) static pressures on the axisymmetric body with fairwater (AFF-2-P-)

(e) wall shear stresses on the axisymmetric body with fairwater (AFF-2-S-)

(f) static pressure across the entire cross-section plane at the three velocity measurement planes

(i) AFF-2-PP-0.904

(ii) AFF-2-PP-0.978

(iii) AFF-2-PP-1.096

3. Body with stern appendages (AFF-3-)

For this configuration, only the four aft-most measurement planes (0.978, 1.040, 1.096 and 1.200) will require measurement. Here, the profiles at constant radius will be the same as for the fairwater configuration (2).

(a) three components of mean and turbulence velocities, and axial-radial and axial-tangential Reynolds stresses across the four planes designated as

(i) AFF-3-V-0.978

(ii) AFF-3-V-1.040

(iii) AFF-3-V-1.096

(iv) AFF-3-V-1.200

Measurement locations r/R_{max} will be similar to the case of (2).

(b) static pressure around the appendage/hull intersection region (pressure tap locations AH1 to AH41 of Reference 14) designated as

(i) AFF-3-P:AH

(c) static pressure at the pressure tap locations of SA1 to SA33 of the stern appendage as specified in Reference 14 designated as AFF-3-P:SA

(d) static pressure across the entire cross-section plane at the three velocity measurement planes

(i) AFF-3-PP-0.978

(ii) AFF-3-PP-1.040

(iii) AFF-3-PP-1.096

(e) repeat (3a) at AP plane for two additional appendage locations, one upstream and one downstream of the baseline location

(i) AFF-3-V:AU-0.978 four stern appendages upstream of the baseline location

(ii) AFF-3-V:AD-0.978 four stern appendages downstream of the baseline location

4. Body with fairwater and at angle of attack of 2 degrees (AFF-4-)

(a) boundary layer measurements will be made at $\theta = 0°$ at the axial locations

(i) AFF-4-VP-0.840

(ii) AFF-4-VP-0.904

(iii) AFF-4-VP-0.978

and the standard wake survey will be made at the axial locations

(i) AFF-4-V-0.904

(ii) AFF-4-V-0.978

(iii) AFF-4-V-1.096

Axial, radial and tangential mean and turbulence velocities, and axial-radial and axial-tangential Reynolds stresses will be measured. Here, the fairwater will be set at an upright position with 2° bow up and at a port side position with 2° to the port. Measurement locations r/R_{max} will be similar to the case of (2).

(b) static pressure around the fairwater/hull intersection region (pressure tap locations FH1 to FH76 of Reference 14) designated as AFF-4-P:FH.

(c) static pressure at the pressure tap locations of FW1 to FW30 of the bridge fairwater designated as AFF-4-P:FW

5. Body with fairwater and at angle of drift of 2 degrees (AFF-5-)

(a) for this configuration, the boundary layer velocity profiles will be made at $\theta = 0°$, $\pm 45°$ at the same boundary layer axial locations as in (4), i.e.,

(i) AFF-5-VP-0.840

(ii) AFF-5-VP-0.904

(iii) AFF-5-VP-0.978.

The standard wake survey will also be made at the same wake survey axial locations as in (4), i.e.

(i) AFF-5-V-0.904

(ii) AFF-5-V-0.978

(iii) AFF-5-V-1.096.

Axial, radial and tangential mean and turbulence intensities, and axial-radial and axial-tangential Reynolds stresses will be measured. Here the fairwater will be set at a port side position with body angle of drift at $\pm 2°$. Measurement locations r/R_{max} will be similar to the case of (2).

(b) static pressure around the appendage/hull intersection region (pressure tap locations FH1 to FH76) designated as AFF-5-P:FH

(c) static pressure at the pressure locations of FW1 to FW30 of the bridge fairwater designated as AFF-5-P:FW

6. Body with ring wing 1 (AFF-6-)

(a) boundary layer profile along a line $\theta = 0$ degrees will consist of:

AFF-6-V-0.978 r/R_{max} = 0.22, 0.246, 0.286, 0.325, 0.52, 0.53, 0.54, 0.55, 0.56, 0.58, 0.60, 0.702, 0.830, 0.979, 1.167, 1.385, 1.652, 1.969, 2.0 and 2.25

AFF-6-V-0.997 r/R_{max} = 0.22, 0.25, 0.30, 0.35, 0.37, 0.38, 0.39, 0.40, 0.41, 0.42, 0.44, 0.46, 0.48, 0.50, 0.52, 0.54, 0.55, 0.56, 0.57, 0.58, 0.59, 0.60, 0.62, 0.65, 0.70, 0.75, 0.80, 0.90, 1.00, 1.25, 1.50, 1.75, 2.0, 2.25, 2.50

(b) mean axial and radial velocities, three components of turbulence intensities, and axial-radial Reynolds stress at the AP (x = 13.977 ft = 4.260 m, x/L = 0.978) and exit (x = 14.249 ft = 4.343 m, x/L = 0.997), and three planes downstream of the ring wing (x/L = 1.040, 1.096 and 1.20) (AFF-6-V-)

(i) AFF-6-V-0.978 r/R_{max} = 0.22, 0.25, 0.30, 0.35, 0.38

(ii) AFF-6-V-0.997 r/R_{max} = 0.22, 0.25, 0.30, 0.35, 0.40, 0.45, 0.50, 0.60

(iii) AFF-6-V-1.040

(iv) AFF-6-V-1.096 r/R_{max} = 0.22, 0.25, 0.30, 0.35, 0.40, 0.45, 0.50, 0.60, 0.72

(v) AFF-6-V-1.200

(c) static pressure along the inner and outer surfaces of ring wing 1 (pressure tap locations W1U1 to W1U19 on the upper meridian of the duct, three additional pressure taps at lower, port and starboard meridians at wing pressure tap stations 4, 6, 8, 13, 15, and 17) and static pressure on the upper meridian of the hull (HU18, HU19, HU20 and HU21) AFF-6-P-S1

7. Body with ring wing 2 (AFF-7-)

(a) boundary layer profiles along a line $\theta = 0$ degrees will be same as 6 except where interference of probe and model prevent the measurement.

(b) The standard wake surveys at constant radius will be at the following locations:

(i) AFF-7-V-0.978 r/R_{max} = 0.22, 0.25, 0.30, 0.35, 0.38

(ii) AFF-7-V-0.996 r/R_{max} = 0.22, 0.25, 0.30, 0.38, 0.45, 0.50, 0.60

(iii) AFF-7-V-1.040

(iv) AFF-7-V-1.096 r/R_{max} = 0.22, 0.25, 0.30, 0.35, 0.40, 0.45, 0.50, 0.60, 0.72

(v) AFF-7-V-1.200

(c) static pressure along the inner and outer surfaces of ring wing 2 on the upper meridian of the duct, three additional pressure taps at lower, port and starboard meridians at wing pressure tap stations 4, 6, 8, 13, 14 and 17 and static pressure on the upper meridian of the hull (HU18, HU19 and HU21) AFF-7-P:S2 and AFF-7-P.

8. Axisymmetric body with fairwater and the four symmetric stern appendages at zero angle of attack and zero drift (AFF-8-)

(a) axial, radial and tangential mean and turbulence velocities, and axial-radial and axial-tangential Reynolds stresses across the three planes designated as

(i) AFF-8-V-0.978

(ii) AFF-8-V-1.040

(iii) AFF-8-V-1.096

r/R_{max} measurement locations will be similar to the case of (2). Here the fairwater will be set at an upright position and the baseline appendage configuration will be used.

(b) static pressure across the entire cross-section plane at the three velocity measurement planes

(i) AFF-8-PP-0.978

(ii) AFF-8-PP-1.040

(iii) AFF-8-PP-1.096

9. Time-varying wake harmonic measurements: The rationale and background of time-varying wake harmonic and wake spectra are discussed in the Appendix. The measurement plane will be at $x/L = 0.978$ for $r/R_{max} = 0.30$, 0.40 and 0.50. Model configurations are the bare hull, bare hull with fairwater , bare hull with baseline stern appendage, bare hull with ring wing 1, bare hull with ring wing 2, and fully appended model.

10. The spatial variation (wake harmonics) of mean velocities (u_x, v_r, w_θ) at the AP ($r/R_{max} = 0.978$) will be analyzed for all model configurations tested (refer to RUN I.D. from AFF-1-V-0.978 to AFF-8-V-0.978). The measurements of $u_x(\theta)$, $v_r(\theta)$, $w_\theta(\theta)$ at a given r/R_{max} will be used to determine the values of the wake harmonic amplitudes A_{un}, A_{vn}, A_{wn}, B_{un}, B_{vn}, B_{wn} for n = 1, 2,... N. The experimental accuracy of determining the wake harmonic amplitudes at high harmonics will be assessed.

A summary of all test conditions for AFF tests is presented in Table 3.

TMB TEST PLAN

In the following, specifications are provided for measuring the body normal and longitudinal forces, pitching and yawing moments and stock torque and spanwise center of pressure of the stern appendage of the five model configurations to be tested in the DTRC deep-water towing basin (TMB):

1. Axisymmetric body (DTRC Model No. 5470)

(a) longitudinal and lateral force coefficients and yaw moment coefficient for body angle of drift from -4 to +18°

TMB-1-F-α = 0; β = ...

2. Axisymmetric body with bridge fairwater

(a) longitudinal and normal force coefficients and pitching moment coefficient for body angle of attack from -8 to +18°

TMB-2-F-α = ...; β = 0 (α = 0°, + 2° must be included)

(b) longitudinal and normal force coefficients and pitching moment coefficient for body angle of drift from -4 to +18° (fairwater attached to bottom of model).

TMB-2-F-α = 0; β = ... (β = 0°, +2° must be included)

3. Axisymmetric body with four identical stern appendages

(a) longitudinal and lateral force coefficients and yaw moment coefficient for body angle of drift from -4 to +18°

TMB-3-F-α = 0; β = ... ; γ = 0

4. Axisymmetric body with both bridge fairwater and four identical stern appendages

(a) longitudinal and lateral force coefficients, yaw moment coefficient and lift, drag and stock torque for:

(i) the lower rudder (opposite to the fairwater)

TMB-8-F-α = 0; β1 = ...

(ii) the upper rudder (behind the fairwater)

TMB-8-F-α = 0; $\beta 2$ = ...

for the body angle of drift from -4 to +18° (fairwater attached to starboard side of model)

(b) longitudinal and normal force coefficients and pitching moment coefficient and lift/drag and stock torque for the starboard sternplane for body angle of attack from -8 to +18° (fairwater attached to bottom of model)

TMB-8-F-α = ... ; β = 0; γ = 0

(c) longitudinal and normal force coefficients and pitching moment coefficient and lift/drag and stock torque for the starboard sternplane for stern plane angle of incidence γ from -15 to +15° for body angle of attack from -8 to +18° (fairwater attached to bottom of model)

TMB-8-F-α = ...; β = 0; γ = ... (γ = 5° must be included)

(d) longitudinal force coefficients for forward speeds from 2 to 8 knots at zero angle of attack and drift

TMB-8-F-$\alpha = \beta = \gamma$ = 0; U_0 = ... knots

5. Axisymmetric body with ring wing 1

(a) longitudinal and lateral force coefficients and yaw moment coefficient for body angle of drift from -4° to + 18°

TMB-6-F-α = 0; β = ...

6. Resistance measurement at zero angle of attack and drift will be measured and designated as

TMB-1-R-H	axisymmetric body DTRC Model No. 5470
TMB-2-R-FWH	axisymmetric body with fairwater
TMB-3-R-SAH	axisymmetric body with four identical stern appendages
TMB-6-R-SH1H	axisymmetric body with ring wing 1
TMB-7-R-SH2H	axisymmetric body with ring wing 2
TMB-8-R-FWSAH	axisymmetric body with both fairwater and stern apendages

A summary of all test conditions is presented in Table 4.

HSMB TEST PLAN

A series of resistance stripping tests and planar motion mechanism static tests are scheduled for Model 5470 in a deeply submerged condition. This series of tests examines various model conditions as follows:

(A) Resistance Stripping Tests

axisymmetric body (HSMB-1-R)

axisymmetric body with fairwater (HSMB-2-R)

axisymmetric body with four identical stern appendages (HSMB-3-R)

axisymmetric body with ring wing 1 (HSMB-6-R)

axisymmetric body with ring wing 2 (HSMB-7-R)

axisymmetric body with fairwater and four stern appendages (HSMB-8-R)

(B) PMM Statics Tests

(1) vertical plane statics: $-20° \leq \alpha \leq 20°$

(a) axisymmetric body (HSMB-1-F-α)

(b) axisymmetric body with ring wing 1 (HSMB-6-F-α)

(2) horizontal plane statics: $-20° \leq \beta \leq 20°$

(a) axisymmetric body with fairwater (HSMB-2-F-β)

(b) axisymmetric body with ring wing 1 (HSMB-6-F-β)

where α is the angle of attack and β is the angle of drift. The test speed used in the program is in the range of 5 - 10 ft/sec for the stripping tests and the PMM statics are conducted for Reynolds number 1.2×10^7 based on the model length.

A summary of all HSMB tests is presented in Table 5.

ACKNOWLEDGEMENTS

The authors would like to thank Mr. Gary Jones of the DARPA Submarine Technology Office for his support of this project. We also thank Dr. L. Patrick Purtell, Dr. Jerome P. Feldman, Mr. William G. Day, Dr. Ming S. Chang and Mr. Scott Gowing for their contribution to and participation in this project.

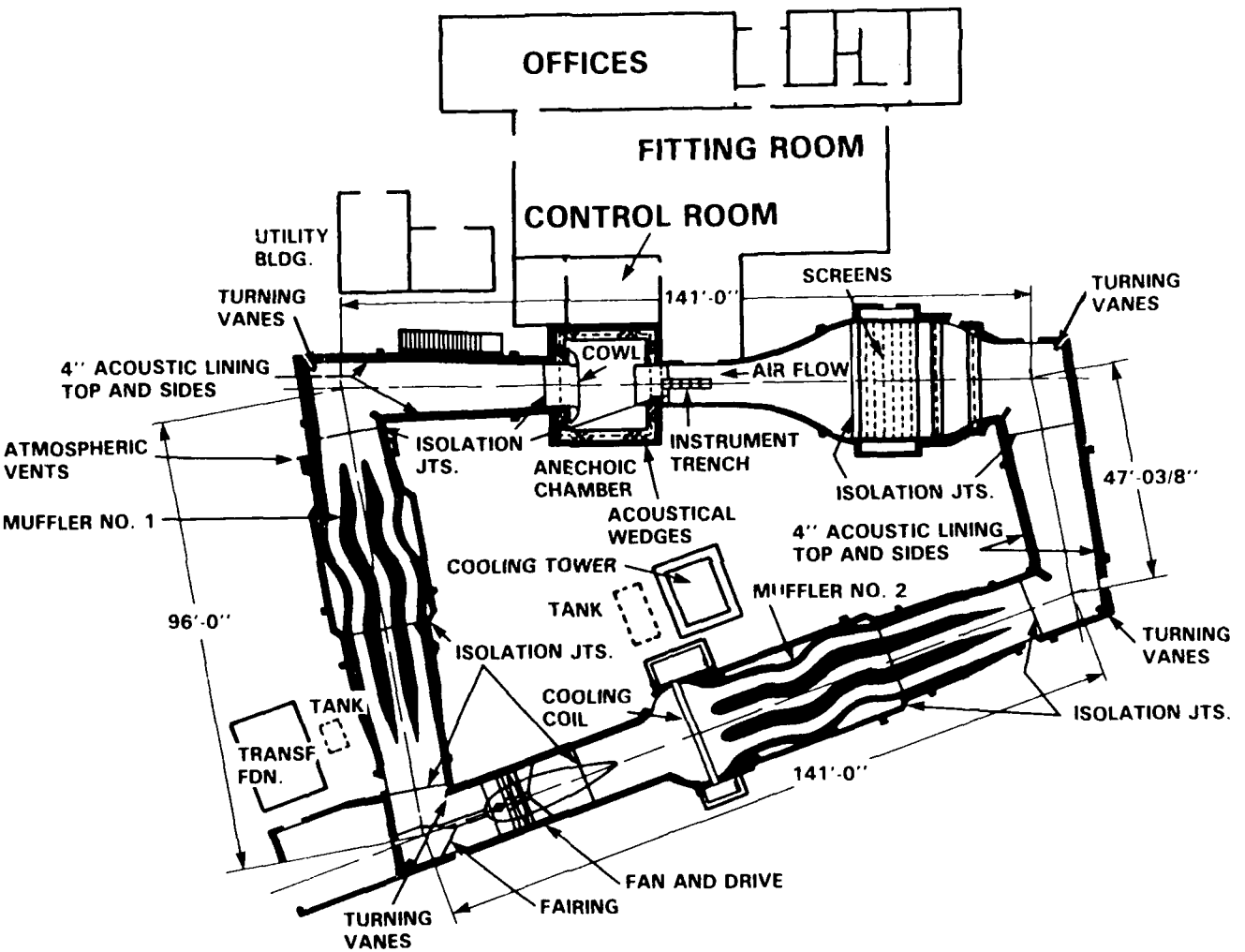

Fig. 1. Schematic of Anechoic Flow Facility (AFF).

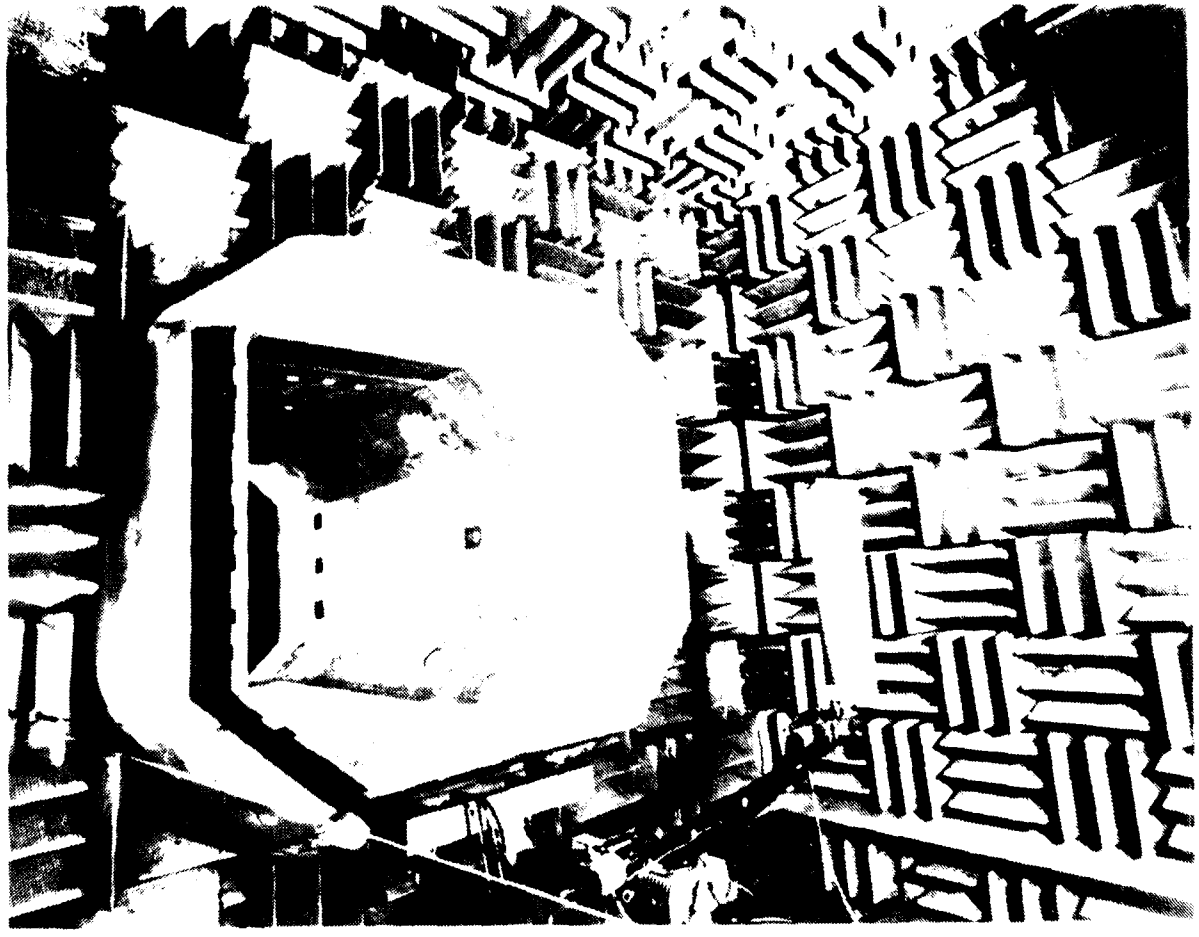

Fig. 2. Anechoic Flow Facility Test Section
2a. Closed- and open-jet Test Section

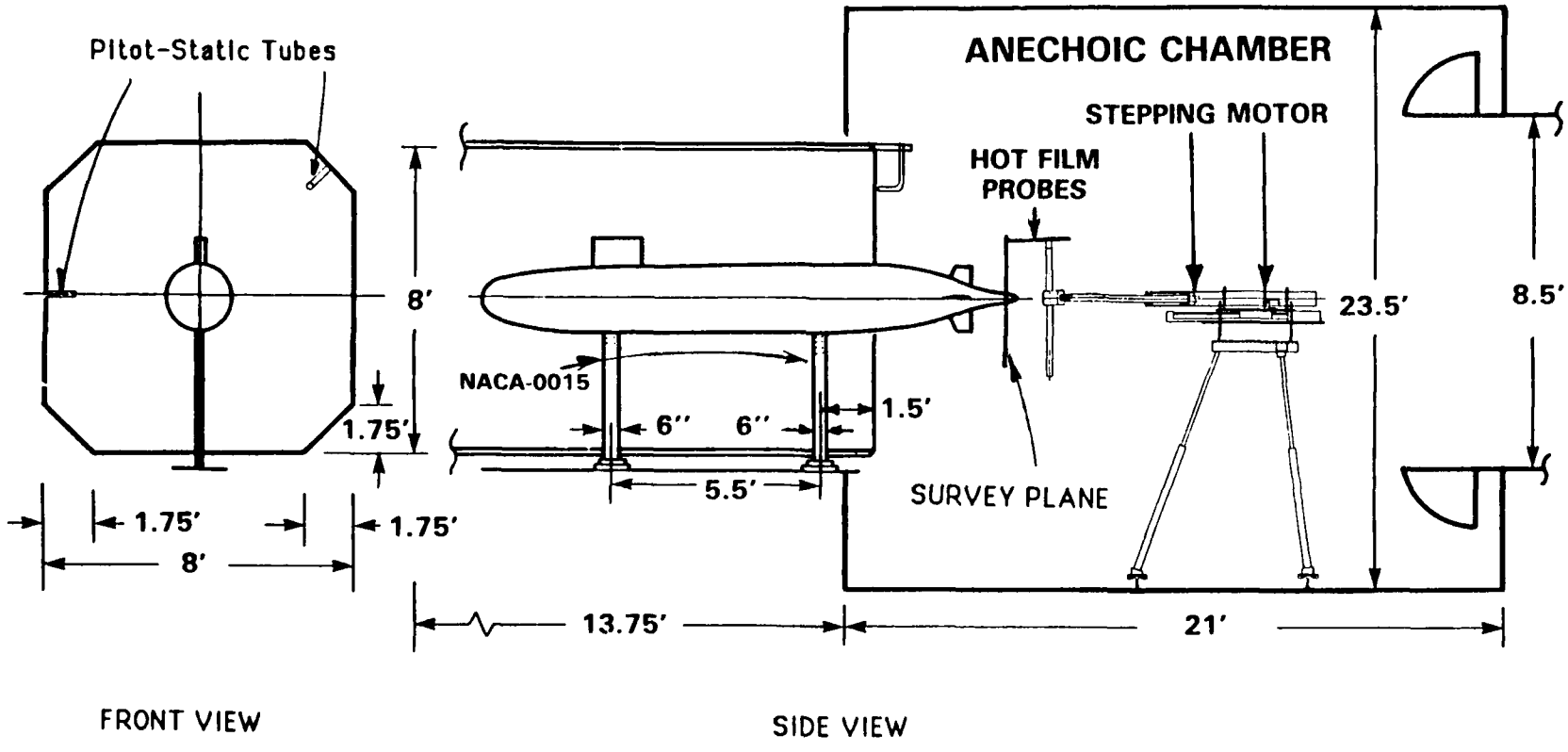

2b. Side View of Model in closed- and open-jet test section

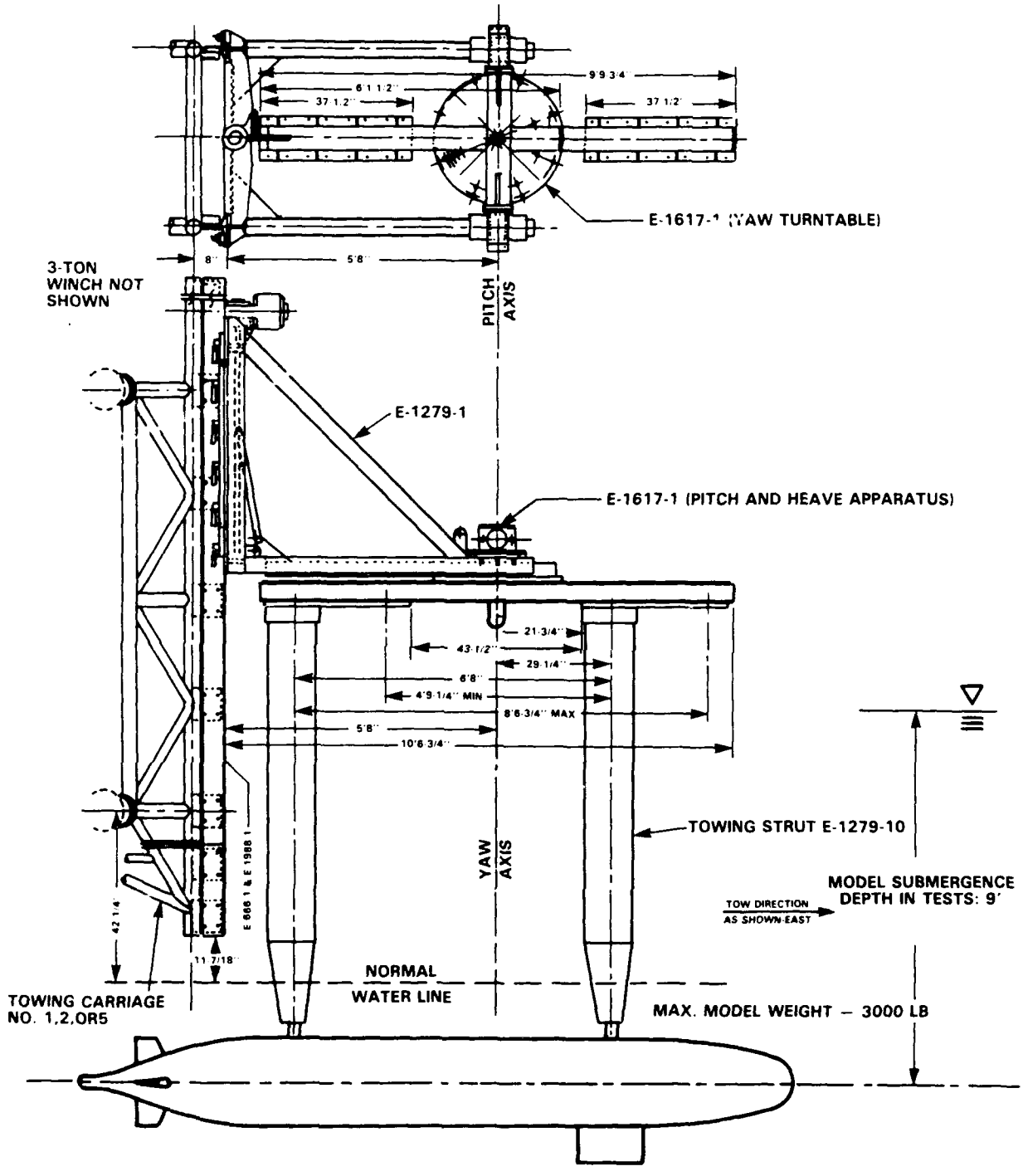

Fig. 3. Model mounted in DTRC Towing Tank (TMB)

3a. Planer motion mechanism at DTRC Towing Tank (TMB)

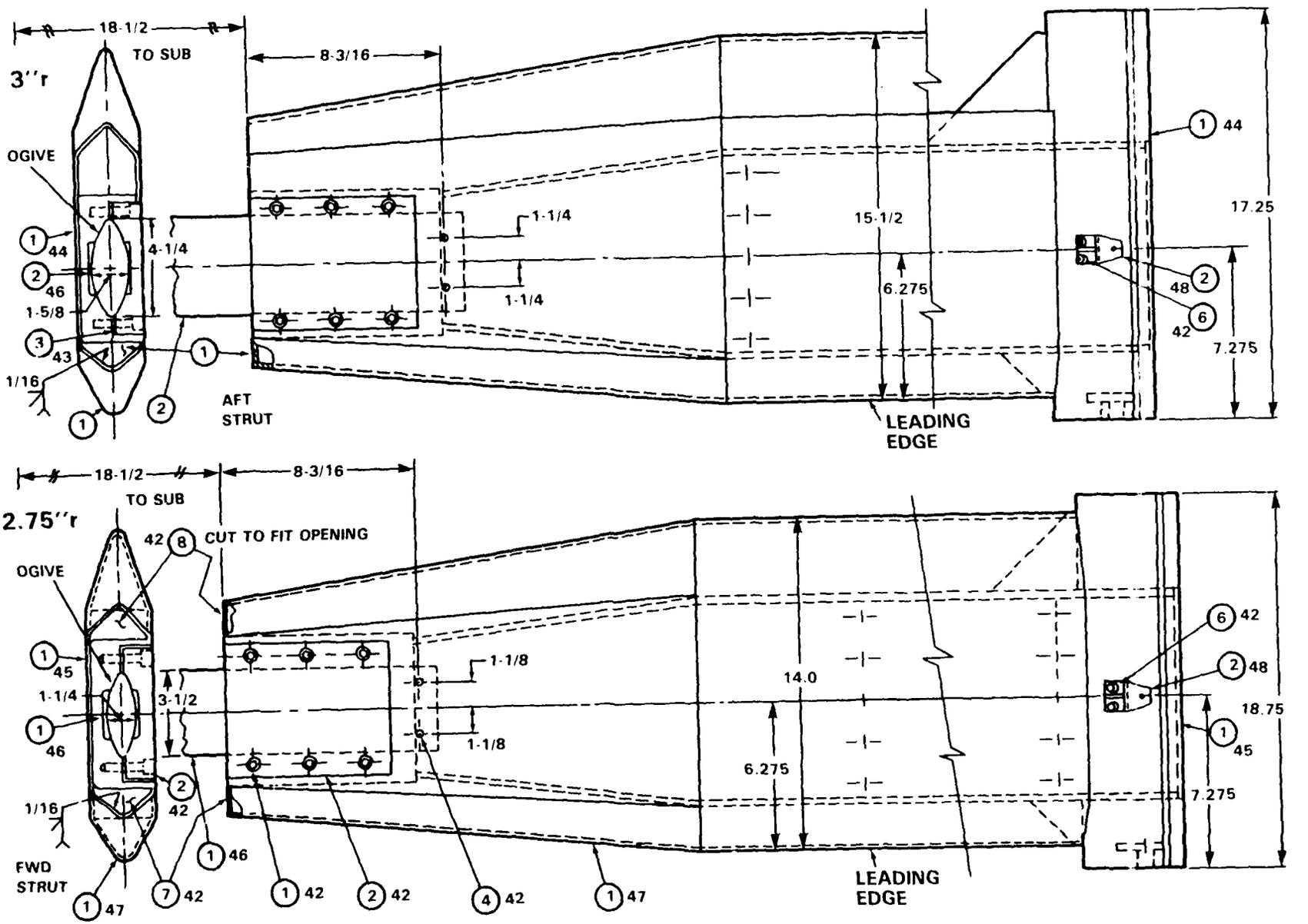

Fig. 3b. Struts used in the DTRC PMM System

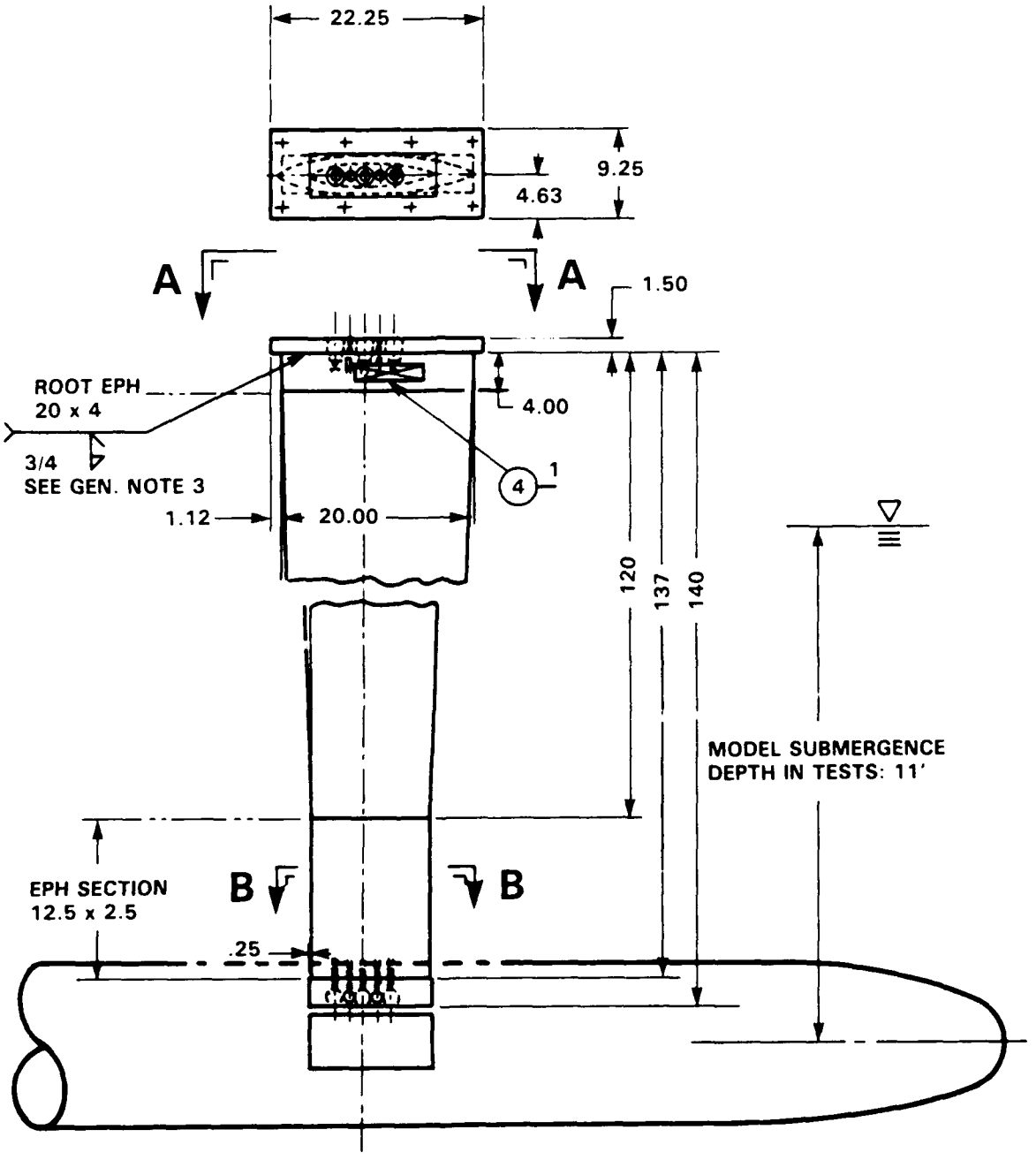

Fig. 4a. Strut used for resistance tests at DTRC Towing Tank

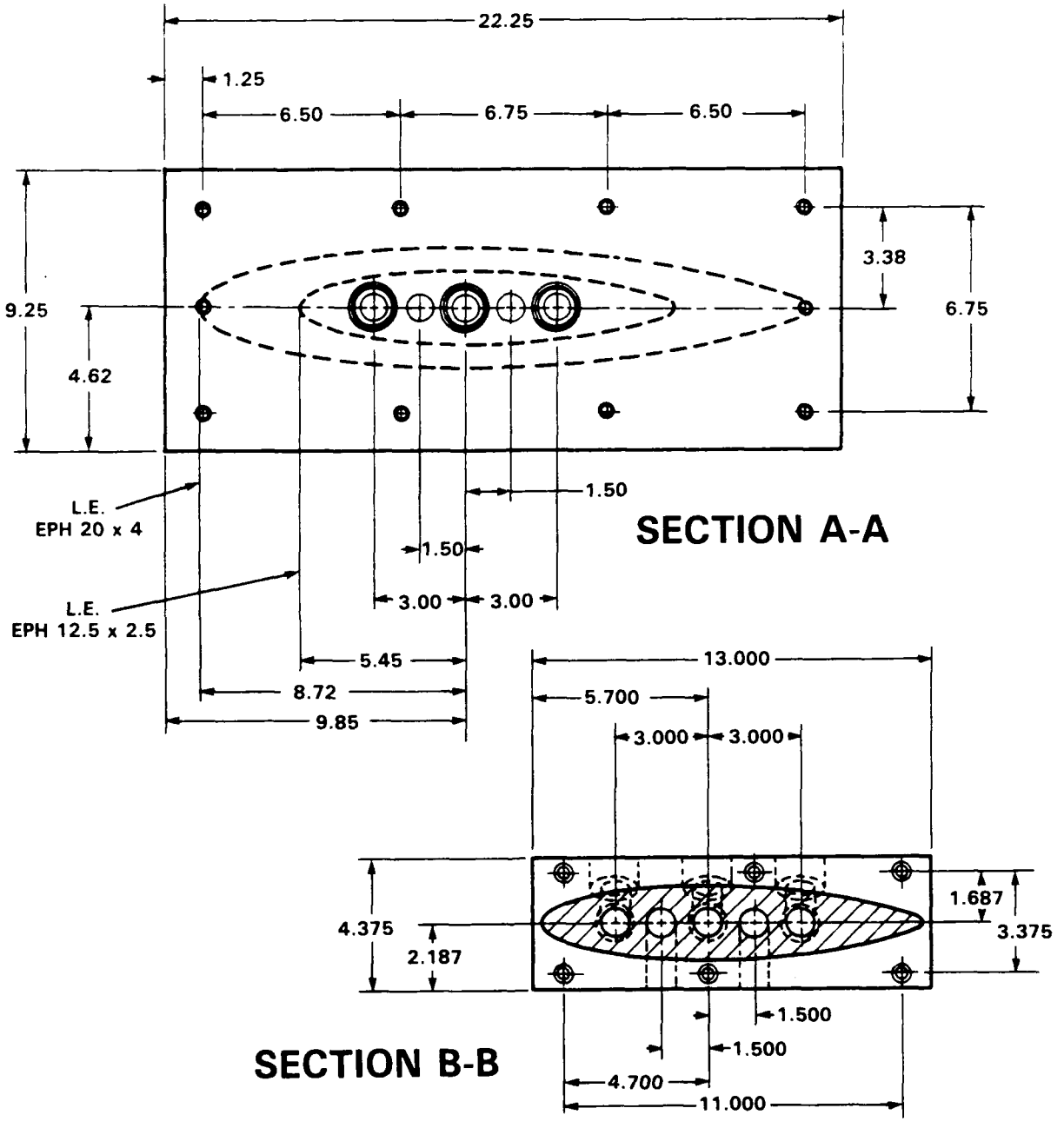

Fig. 4b. Strut used for resistance tests at DTRC Towing Tank

Table 1. Cryptic Test Notation

The cryptic test notation **A - B - C - D - E - F** designates the following conditions:

A designates test facility as follows:
- AFF for DTRC Anechoic Flow Facility
- TMB for DTRC deep-water towing basin
- HSMB for Tracor Hydronautics Ship Model Basin

B designates model configuration as follows:
1. for axisymmetric body at zero angle of attack and zero drift
2. for axisymmetric body with fairwater at zero angle of attack and zero drift
3. for axisymmetric body with four identical stern appendages at zero angle of attack and zero drift
4. for axisymmetric body with fairwater at angle of attack and zero drift
5. for axisymmetric body with fairwater at drift and zero angle of attack
6. for axisymmetric body with ring wing 1 at zero angle of attack and zero drift
7. for axisymmetric body with ring wing 2 at zero angle of attack and zero drift
8. for axisymmetric body with fairwater and four identical stern appendages at zero angle of attack and zero drift

C designates type of data collected as follows:
- V for velocity profile/wake data including 3-component mean velocity data (u_x/U_{ref}, v_r/U_{ref}, w_θ/U_{ref}), turbulence fluctuation data ($\sqrt{u_x'^2}/U_{ref}$, ($\sqrt{v_r'^2}/U_{ref}$, ($\sqrt{w_\theta'^2}/U_{ref}$), and turbulence intensity data ($\overline{-u_x'v_r'}/U_{ref}^2$, $\overline{-u_x'w_\theta'}/U_{ref}^2$)
- P for static wall pressure data for axisymmetric hull
- P:FH for static wall pressure data for fairwater/hull intersection region
- P:AH for static wall pressure data for stern appendage/hull intersection region
- P:FW for static wall pressure data for fairwater
- S for shear stress coefficients
- PP for profiles of static pressure coefficients
- F for force moment coefficient
- R for resistance measurements
- FV for flow visualization

D designates a body location or condition indicator as follows:
for AFF facility, this indicates axial position as a fraction of total body length on axisymmetric body, x/L
for TMB facility, this indicates body angle of attack.

E designates a body location or condition indicator as follows:
for AFF facility, this indicates radial position as a fraction of maximum hull radius of the axisymmetric body, r/R_{max}
for TMB facility, this indicates body angle of drift

F designates the angular position on the axisymmetric body defined positive clockwise with respect to the 0 degree (12 o'clock) position, viewing from bow toward stern

Table 2. Radial Locations for Measurements

i	$(r_i-r_o)/\delta_r$	i	$(r_i-r_o)/\delta_r$
1	0.01	11	0.32
2	0.022	12	0.40
3	0.036	13	0.49
4	0.05	14	0.59
5	0.07	15	0.72
6	0.10	16	0.87
7	0.13	17	1.06
8	0.17	18	1.28
9	0.21	19	1.55
10	0.26	20	1.87

Table 3. Summary of Experiments in DTRC AFF (Model 5471)

RUN I.D.	MEASURED QUANTITIES	MEASUREMENT LOCATION	MODEL CONFIGURATION
AFF-1-VP-0.741 0.781 0.805 0.840 0.857 0.904 0.927 0.956 0.978	boundary layer velocity profiles† u_x/U_{ref} , v_r/U_{ref} u'_x/U_{ref} , v'_r/U_{ref} , w'_θ/U_{ref} $\overline{u'_x v'_r}\ /U^2_{ref}$	20 radial locations defined by Table 2 and δ_r/R_{max} = 0.36 0.40 0.42 0.44 0.54 } $\theta = 0°, \pm 45°$ 0.72 0.84 0.94 0.99 } $\theta = 0°, \pm 45°, \pm 90°$	AFF-1 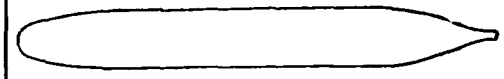
AFF-1-V-0.904 AFF-1-V-0.978 1.040 1.096 1.200	wake surveys†† u_x/U_{ref} , v_r/U_{ref} , w_θ/U_{ref} u'_x/U_{ref} , v'_r/U_{ref} , w'_θ/U_{ref} $\overline{-u'_x v'_r}\ /U^2_{ref}$, $\overline{-u'_x w'_\theta}\ /U^2_{ref}$	r /R_{max} = 0.45, 0.50, 0.60, 0.72,. 0.92, 1.20 r/R_{max} = 0.25, 0.30, 0.35, 0.40, 0.50 0.60, 0.72, 0.92, 1.20, 2.00	
AFF-1-P AFF-1-P:FH AFF-1-P:AH	static wall pressure	for all H series taps 1 to 21 for all FH series taps on the hull for all AH series taps on the hull	
AFF-1-S	wall shear stress	for all H series taps 8 to 21	

† velocity data at constant angle θ, varying radius

†† velocity data at varying angle θ ($|180°| \le \theta$), constant radius, $\Delta\theta = 1°$ for $\theta \le |20°|$ and $\Delta\theta = 2°$ otherwise

Table 3. (cont'd) Summary of Experiments in DTRC AFF (Model 5471)

RUN I.D.	MEASURED QUANTITIES	MEASUREMENT LOCATION	MODEL CONFIGURATION
AFF-1-PP-0.840	static pressure profiles	$\theta = 0°$, same r/R_{max} as AFF-1-VP	
AFF-1-PP-0.904 0.978 1.040 1.096	static pressure survey	same r/R_{max} as AFF-1-V	
AFF-2-VP-0.840	boundary layer velocity profiles same as AFF-1-VP	same as AFF-1-VP	AFF-2
AFF-2-V-0.840	wake surveys	r/R_{max} = 0.82, 0.93, 1.28; $\lvert 45° \rvert < \theta$	
AFF-2-V-0.904	u_x/U_{ref} , v_r/U_{ref} , w_θ/U_{ref}	r/R_{max} = 0.45, 0.50, 0.60, 0.72, 0.92. 1.20, 1.60, 2.00	
AFF-2-V-0.978 1.040 1.096 1.200	u'_x/U_{ref} , v'_r/U_{ref} , w'_θ/U_{ref} $\overline{-u'_x v'_r}/U^2_{ref}$, $\overline{-u'_x w'_\theta}/U^2_{ref}$	r/R_{max} = 0.25, 0.30, 0.35, 0.40, 0.50 0.60, 0.72, 0.92, 1.20, 1.60, 2.00	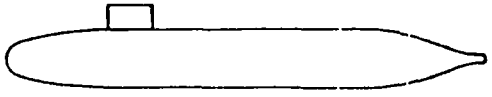
AFF-2-P AFF-2-P:FH AFF-2-P:FW	static wall pressure	for all H series taps 1 to 21 for all FH series taps 1 to 76 for all FW series taps 1 to 30	
AFF-2-S	wall shear stress	for all H series taps 8 to 21	
AFF-2-PP-0.904 0.978 1.096	static pressure survey	same r/R_{max} as AFF-2-V	
AFF-3-V-0.978 1.040 1.096 1.200	wake surveys same as AFF-2-V	same r/R_{max} as AFF-2-V	AFF-3

Table 3. (cont'd) Summary of Experiments in DTRC AFF (Model 5471)

RUN I.D.	MEASURED QUANTITIES	MEASUREMENT LOCATION	MODEL CONFIGURATION
AFF-3-P:AH AFF-3-P:SA	static wall pressure	for all AH series taps 1 to 41 for all SA series taps 1 to 33	
AFF-3-PP-0.978 1.040 1.096	static pressure survey	same r/R_{max} as AFF-2-V	
AFF-3-V:AU-0.978 AFF-3-V:AD-0.978	wake surveys same as AFF-2-V	same r/R_{max} as AFF-2-V	
AFF-4-VP-0.840 0.904 0.978	boundary layer velocity profiles	same r/R_{max} as AFF-1-VP, $\theta = 0°, \pm 45°$	AFF-4
AFF-4-V-0.904 0.978 1.096	wake surveys same as AFF-2-V	same r/R_{max} as AFF-2-V	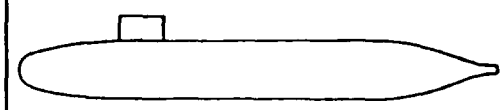
AFF-4-P:FH AFF-4-P:FW	static wall pressure	for all FH series taps 1 to 76 for all FW series taps 1 to 30	with angle of attack of $\alpha = +2°$
AFF-5-VP-0.840 0.904 0.978	boundary layer velocity profiles	same r/R_{max} as AFF-1-VP, $\theta = 0°$, $\pm 45°$	AFF-5
AFF-5-V-0.904 0.978 1.096	wake surveys same as AFF-2-V	same r/R_{max} as AFF-2-V	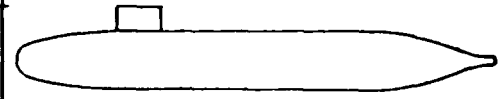
AFF-5-P:FH AFF-5-P:FW	static wall pressure	for all FH series taps 1 to 76 for all FW series taps 1 to 30	with angle of drift of $\beta = +2°$

Table 3. (cont'd) Summary of Experiments in DTRC AFF (Model 5471)

RUN I.D.	MEASURED QUANTITIES	MEASUREMENT LOCATION	MODEL CONFIGURATION
AFF-6-VP-0.978	boundary layer velocity profiles same as AFF-1-VP	r/R_{max} = 0.220, 0.246, 0.286, 0.325, 0.520, 0.530, 0.540, 0.550, 0.560, 0.580, 0.600, 0.702, 0.830, 0.979, 1.167, 1.385, 1.652, 1.969, 2.000, 2.250	AFF-6
0.997		r/R_{max} = 0.22, 0.25, 0.30, 0.35, 0.37, 0.38, 0.39, 0.40, 0.41, 0.42, 0.44, 0.46, 0.48, 0.50, 0.52, 0.54, 0.55, 0.56, 0.57, 0.58, 0.59, 0.60, 0.62, 0.65, 0.70, 0.75, 0.80, 0.90, 1.00, 1.25, 1.50, 1.75, 2.00, 2.25, 2.50 $\theta = 0°$	
AFF-6-V-0.978	wake survey	r/R_{max} = 0.22, 0.25, 0.30, 0.35, 0.38	Ring Wing 1
0.997	same as AFF-1-V	r/R_{max} = 0.22, 0.25, 0.30, 0.35, 0.40, 0.45, 0.50, 0.60	
1.040 1.096 1.200		r/R_{max} = 0.22, 0.25, 0.30, 0.35, 0.40, 0.45, 0.50, 0.60, 0.72	
AFF-6-P:S1 AFF-6-P	static wall pressure	for all W1 series taps (37 total) for all HU series taps HU18 to HU21	
AFF-7-VP-0.978 AFF-7-VP-0.996	boundary layer velocity profiles same as AFF-1-VP	same as AFF-6-VP except use x/L = 0.996 instead of 0.997	AFF-7
AFF-7-V-0.978 0.996	wake surveys	same as AFF-6-V r/R_{max} = 0.22, 0.25, 0.30, 0.38, 0.45, 0.50, 0.60	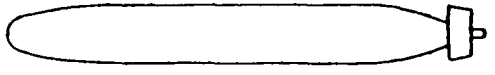
1.040 1.096 1.200	same as AFF-1-V	same as AFF-6-V	Ring Wing 2

Table 3. (cont'd) Summary of Experiments in DTRC AFF (Model 5471)

RUN I.D.	MEASURED QUANTITIES	MEASUREMENT LOCATION	MODEL CONFIGURATION
AFF-7-P:S2 AFF-7-P	static wall pressure	for all W2 series taps (37 total) for all HU series taps HU18 to HU21	
AFF-8-V-0.978 AFF-8-V-1.040 AFF-8-V-1.096	wake surveys same as AFF-2-V	same as AFF-2-V	AFF-8 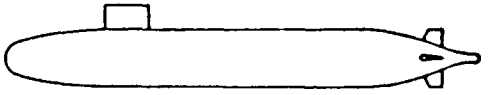
AFF-8-PP-0.978 AFF-8-PP-1.040 AFF-8-PP-1.096	static pressure survey	same as AFF-2-PP	
AFF-1-V-0.978 AFF-2-V-0.978 AFF-3-V-0.978 AFF-6-V-0.978 AFF-7-V-0.978 AFF-8-V-0.978	time-varying 5th wake-harmonic	5 1-D probes every $\Delta\theta = 360°/5$ with a second set of 5 probes located $\Delta\theta/4$ from the first. $r/R_{max} = 0.30, 0.40, 0.50$	

Table 4. Summary of Experiments in DTRC TMB (Model 5470)

RUN I.D.	MEASURED QUANTITIES	MEASUREMENT CONDITIONS	MODEL CONFIGURATION
TMB-1-F-β	force and moment coefficients	$-4° \le \beta \le 18°$; $\alpha = 0°$, $\gamma = 0°$	see AFF-1
TMB-2-F-α β	force and moment coefficients	$-8° \le \alpha \le 18°$; $\beta = 0°$, $\gamma = 0°$ $-4° \le \beta \le 18°$; $\alpha = 0°$, $\gamma = 0°$	see AFF-2
TMB-3-F-β	force and moment coefficients	$-4° \le \beta \le 18°$; $\alpha = 0°$, $\gamma = 0°$	see AFF-3
TMB-6-F-β	force and moment coefficients	$-4° \le \beta \le 18°$, $\alpha = 0°$, $\gamma = 0°$	see AFF-6
TMB-8-F-β1 β2	force, moment, lift, drag and stock torque	lower vertical plane $-4° \le \beta_1, \beta_2 \le 18°$ upper vertical plane $\alpha = 0°$, $\gamma = 0°$	see AFF-8
TMB-8-F-α	force, moment, lift, drag and stock torque	starboard stern plane $-8° \le \alpha \le 18°$; $\beta = 0°$, $\gamma = 0°$	
TMB-8-F-$\alpha\gamma$	force, moment, lift, drag and stock torque	starboard sternplane $-8° \le \alpha \le 18°$, $-15° \le \gamma \le 15°$, $\beta = 0°$	
TMB-8-F-U_o	longitudinal force	$2 \le U_o \le 8$ knots, $\alpha = 0°$, $\beta = 0°$, $\gamma = 0°$	
TMB-1-R-H TMB-2-R- FWH TMB-3-R- SAH TMB-6-R-SH1H TMB-7-R-SH2H TMB-8-R-FWSAH	resistance		see AFF-1 see AFF-2 see AFF-3 see AFF-6 see AFF-7 see AFF-8

Table 5. Summary of Experiments in
the Tracor Hydronautics Ship Model Basin (HSMB) (Model 5470)

RUN I.D.	MEASURED QUANTITIES	MEASUREMENT CONDITIONS	MODEL CONFIGURATION
HSMB-1-R-H	resistance		see AFF-1
HSMB-2-R-FWH	resistance		see AFF-2
HSMB-3-R-SAH	resistance		see AFF-3
HSMB-6-R-SH1H	resistance		see AFF-6
HSMB-7-R-SH2H	resistance		see AFF-7
HSMB-8-R-FWSAH	resistance		see AFF-8
HSMB-1-F-α	force and moment coefficients	$\lvert\alpha\rvert \leq 20°$ $\Delta\alpha = 2°$	see AFF-1
HSMB-6-F-α	force and moment coefficients	$\lvert\alpha\rvert \leq 20°$ $\Delta\alpha = 2°$	see AFF-6
HSMB-2-F-β	force and moment coefficients	$\lvert\beta\rvert \leq 20°$ $\Delta\beta = 2°$	see AFF-2
HSMB-6-F-β	force and moment coefficients	$\lvert\beta\rvert \leq 20°$ $\Delta\beta = 2°$	see AFF-6

APPENDIX

WAKE HARMONICS

SPATIAL AND TIME-VARYING

APPENDIX WAKE HARMONICS — SPATIAL AND TIME-VARYING

Spatial wake harmonics of mean velocities (u_x, v_r, w_θ) will be studied at the after perpendicular (AP).

The wake harmonics are represented by

$$\begin{bmatrix} u_x \\ v_r \\ w_\theta \end{bmatrix} = \begin{bmatrix} \overline{u_x} \\ \overline{v_r} \\ \overline{w_\theta} \end{bmatrix} + \sum_{n=1}^{N} \begin{bmatrix} A_{un} \\ A_{vn} \\ A_{wn} \end{bmatrix} \cos n\theta + \sum_{n=1}^{N} \begin{bmatrix} B_{un} \\ B_{vn} \\ B_{wn} \end{bmatrix} \sin n\theta$$

where the cosine coefficients of the nth harmonic are determined by

$$\begin{bmatrix} A_{un} \\ A_{vn} \\ A_{wn} \end{bmatrix} = \frac{1}{\pi} \int_0^{2\pi} \begin{bmatrix} u_x \\ v_r \\ w_\theta \end{bmatrix} \cos n\theta \; d\theta$$

and the sine coefficients by

$$\begin{bmatrix} B_{un} \\ B_{vn} \\ B_{wn} \end{bmatrix} = \frac{1}{\pi} \int_0^{2\pi} \begin{bmatrix} u_x \\ v_r \\ w_\theta \end{bmatrix} \sin n\theta \; d\theta$$

The measurements of $u_x(\theta)$, $v_r(\theta)$ and $w_\theta(\theta)$ at a given r/R_{max} will be used to determine the values of the wake harmonic amplitudes A_{un}, A_{vn}, A_{wn}, B_{un}, B_{vn}, B_{wn} for n = 1, 2, ...N. The experimental accuracy in determining the wake harmonic amplitudes at high harmonics must be assessed.

Time-varying characteristics of the first five (J = 5) wake harmonics at the AP plane will be studied. For the same experimental conditions as those for the spatial harmonics, experiments will be conducted using one set of J = 5 equally circumferentially-spaced one-component hot-film probes. The angle between the adjacent probes is $\Delta\theta = 360/J = 72$ degrees. Another set of 5 equally spaced probes at an angle $\Delta\theta/4 = 18$ degrees from the first set of probes will also be used.

At a given radius, a set of 'a' group single probes located circumferentially at $\theta_j = j\Delta\theta = 0°$, 72°, 144°, 216° and 288°, and another set of 'b' group single probes located at $1/4\,\Delta\theta + j\Delta\theta = 18°$, 90°, 162°, 234° and 306° will be used to measure the axial velocity fluctuations

$$\overline{u'}_{(a,b)j}(t) = u_x\,[t, (1/4\,\Delta\theta) + j\,\Delta\theta] - \overline{U'}\,[(1/4\,\Delta\theta) + j\,\Delta\theta]$$

where the time-average velocities are to be taken for a period T much longer than the time scale of energy containing eddies of the turbulence, $\mathcal{L}$, e.g.,

$$\overline{u_x}\,[(1/4\,\Delta\theta) + j\,\Delta\theta] = \lim_{T>>\mathcal{L}} \frac{1}{T} \int_0^T u_x\,[t, (1/4\,\Delta\theta) + j\,\Delta\theta]\,dt$$

APPENDIX WAKE HARMONICS — SPATIAL AND TIME-VARYING

The hot-film signals of u_x will be collected and stored in a digital computer at a rate of 20 KHz for a period of time T equal to about 60 seconds. The rms velocity fluctuations are

$$\overline{[u'^2_{(a,b)j}]} = \lim_{T>>\mathcal{L}} \frac{1}{T} \int_0^T [u'^2_{(a,b)j}(t)]^2 \, dt = \sigma^2_{(a,b)j}$$

The length microscale of the turbulence λ's are computed using the relation

$$\lambda = [\overline{u'^2} / (\partial u'/\partial t)^2] \, \overline{u'}$$

This relation assumes an isotropic field of turbulence and the assumption of space-time equivalence (Taylor's hypothesis). The turbulence Reynolds number is defined as $R_\lambda = [\overline{u'^2}]^{1/2} \lambda/\nu$, where ν is the kinematic viscosity of the fluid. The axial velocity fluctuations u' include the measurements of both 'a' and 'b' groups. The smallest scales of the turbulence are the Kolmogorov length and time scales, η and τ, respectively. These scales may be established by

$$\eta = (\nu^3/\varepsilon)^{1/4} \cong 1/(15)^{1/4} \, \lambda/R_\lambda^{1/4} \qquad \text{and} \qquad \tau = (\nu/\varepsilon)^{1/2} \cong 1/(15)^{1/2} \, \lambda/\sqrt{\overline{u'^2}}$$

where the turbulence energy dissipation rate ε may be estimated by $\varepsilon = 15\nu (\overline{u'^2}/\lambda^2)$. The correlation coefficient is defined by

$$\rho_{(a,b)j}(t', \theta') = \frac{\overline{u'_{(a,b)}[t, (1/4\,\Delta\theta) + j\,\Delta\theta] \, u'_{(a,b)}[t+t', (1/4\,\Delta\theta) + j\,\Delta\theta + \theta']}}{\left\{\overline{u'^2_{(a,b)}[t, (1/4\,\Delta\theta) + j\,\Delta\theta]}\right\}^{1/2} \left\{\overline{u'^2_{(a,b)}[t,+t' (1/4\,\Delta\theta) + j\,\Delta\theta + \theta']}\right\}^{1/2}}$$

The axial length scales of energy containing eddies may be estimated by

$$l^x_{(a,b)j} = \overline{u_x} \int_0^{T>>\mathcal{L}} \rho_{(a,b)j}(t', \theta' = 0) \, dt'$$

and the circumferential transverse length scales of energy containing eddies may be estimated by

$$l^\theta_{(a,b)j} = r \int_0^{2\pi} \rho_{(a,b)j}(t', \theta') \, d\theta'$$

where the radius r is measured from the body axis. The present measurements will not include the measurements of $\rho_{(a,b)j}(t' = 0, \theta')$ and hence not include the estimates of $l^\theta_{(a,b)j}$. The individual power spectral density of the axial component of the turbulence of the 'a' and 'b' groups measured by J single probes may defined by

APPENDIX WAKE HARMONICS — SPATIAL AND TIME-VARYING

$$S_{(a,b)j}(f) = \lim_{T>>\mathcal{L}} \frac{1}{T} \left| \int_0^T u'_{(a,b)j}(t)\, e^{-i2\pi f\, dt}\, dt \right|^2$$

The averaged turbulence of the 'a' and 'b' groups measured by J single probes are defined by

$$u'_{a/J=5}(t) = 1/J \sum_{j=0}^{J-1} [u'_{aj}(t)] \qquad u'_{b/J=5}(t) = 1/J \sum_{j=0}^{J-1} [u'_{bj}(t)]$$

The amplitude and the phase of the J(=5)th time varying wake harmonics are defined as

$$u'_{J=5}(t) = 1/2\, \{[u'_{a/J=5}(t)]^2 + [u'_{b/J=5}(t)]^2\}^{1/2}$$

$$\theta'_{J=5} = \tan^{-1} [u'_{b/J=5}(t)/u'_{a/J=5}(t)$$

and the averaged rms velocity fluctuations of the Jth time varying wake harmonics are

$$\sigma^2_{J=5} = \lim_{T>>\mathcal{L}} \frac{1}{T} \int_0^T [u'_{J=5}(t)]^2\, dt$$

The power spectral density of the Jth harmonic amplitude and phase are defined as

$$SA_{J=5}(f) = \lim_{T\to\infty} \frac{1}{T} \left| \int_0^T u_{J=5}(t)\, e^{-i2\pi ft}\, dt \right|^2$$

$$\Omega\theta_{J=5}(f) = \text{iim}_{T\to\infty} \frac{1}{T} \left| \int_0^T \theta_{J=5}(t)\, e^{-i2\pi ft}\, dt \right|^2$$

The spectra of $SA_{J=5}(f)$ and $\Omega\theta_{J=5}(f)$ will be determined for $r/R_{max} = 0.30, 0.40$ and 0.50. The nondimensional spectral density is defined as $S_{(a,b)j}(f)\, U_{ref}/[R_{max}\ \sigma_{(a,b)j}]\ S_{A/J=5}(f)\, U_{ref}/[R_{max}\ \sigma^2_{(a,b)j}]$ $SA_{J=5}(f)\, U_{ref}/[R_{max}\ \sigma^2_{(J=5)}]$ and the nondimensional frequency is defined as f_{max}/U_{ref}, where f is the frequency of Hz, R_{max} is the maximum hull radius and U_{ref} is the reference velocity.

REFERENCES

1. Huang, T.T., H.T. Wang, N. Santelli, and N.C. Groves, "Propeller/Stern/Boundary-Layer Interaction on Axisymmetric Bodies: Theory and Experiment," DTNSRDC Report 76-0113, December 1976.

2. Huang, T.T., N. Santelli, and G.S. Belt, "Stern Boundary-Layer Flow on Axisymmetric Bodies," Proceedings of the Twelfth Symposium on Naval Hydrodynamics, 5-9 June 1978, National Academy of Sciences, Washington, DC, pp. 127-157, June 1978.

3. Huang, T.T., N.C. Groves, and G.S. Belt, "Boundary Layer Flow on an Axisymmetric Body with an Inflected Stern," DTNSRDC Report 80/064, June 1980.

4. Groves, N.C., G.S. Belt and T.T. Huang, "Stern Boundary Layer Flow on a Three-Dimensional Body of 3:1 Elliptical Cross Section," DTNSRDC Report 82/022, April 1982.

5. Huang, T.T.and N.C. Groves, "Stern Boundary Layer Flow on a Three-Dimensional Body of 2:1 Elliptical Cross Section," DTNSRDC Report 84/022, October 1984.

6. Huang, T.T.and N.C. Groves, "Effective Wake: Theory and Experiment," Proceedings of the 13th Symposium on Naval Hydrodynamics, Tokyo, Japan, 6-10 October 1980, Shipbuilding Research Association of Japan, pp. 651-673, October 1980.

7. Dickinson, S.C., "An Experimental Investigation of Appendage-Flat Plate Junction Flow, Vol. I: Description, and Vol. II: Elliptical Nose Appendage Data Base, DTNSRDC Report 86/051 and 86/052, December 1986.

8. Davenport, W.J. and R.L. Simpson, "The Turbulence Structure Near an Appendage-Body Junction," paper presented at the 17th Symposium on Naval Hydrodynamics, The Hague, The Netherlands, August 29 - September 2, 1988.

9. Chang, M.S. and L.P. Purtell, "Three-Dimensional Flow Separation and the Effect of Appendages," proceedings of the 16th Symposium on Naval Hydrodynamics, University of California, Berkeley, California, July 13-18, 1986, National Academy Press, pp. 352-370, July 1986.

10. Morgan, W.B. and W.C. Lin, "Computational Fluid Dynamics, Ship Design and Model Evaluation," paper presented at the 4th International Congress of the International Association of East Mediterranean, Varna, pp. 32.1-32.8 , May 1987.

11. Current Capabilities and Future Directions in Computational Fluid Dynamics," prepared by Committee to Assess Current Capabilities and Future Directions in Computational Fluid Dynamics, Aeronautics and Space Engineering Board, Commission on Engineering and Technical Systems, National Research Council, ix+98PP, National Academy Press, Washington, DC (1986).

12. Morgan, W.B. and W.C. Lin, "Computational Fluid Dynamics and Experiments," paper presented at the International Symposium celebrating the 75th Anniversary of the Hamburg Ship Model Basin, September 29, 1988, and will be published in Schifftechnik.

13. "The Influence of Computational Fluid Dynamics on Experimental Aerospace Facilities — A Fifteen Year Projection," National Academy Press, Washington, DC xvi+109PP. (1983).

14. Groves, N.C., T.T. Huang and M.S. Chang, "Geometric Characteristics of DARPA SUBOFF Models (DTRC Model Nos. 5470 and 5471)," Report DTRC/SHD-1298-01, March 1989. AD A210642